Applied Clay Science 53 (2011) 42–47

Contents lists available at ScienceDirect

Applied Clay Science

journal homepage: www.elsevier.com/locate/clay

Research Paper

EPR, FT-IR and XRD investigation of soils from Paraná, Brazil

R.E. Siqueira [a], M.M. Andrade [a], D.F. Valezi [a], C.E.A. Carneiro [b], J.P.P. Pinese [c], A.C.S. da Costa [d], D.A.M. Zaia [b], R. Ralisch [e], W.M. Pontuschka [f], C.L.B. Guedes [a], E. Di Mauro [a,*]

[a] Laboratório de Fluorescência e Ressonância Paramagnética Eletrônica (LAFLURPE), CCE, Universidade Estadual de Londrina, 86051–970, Londrina, PR, Brazil
[b] Departamento de Química-CCE, Universidade Estadual de Londrina, 86051–990, Londrina-PR, Brazil
[c] Departamento de Geociências-CCE, Universidade Estadual de Londrina, 86051–990, Londrina-PR, Brazil
[d] Departamento de Agronomia-CCA, Universidade Estadual de Maringá, 87020–900 Maringá-PR, Brazil
[e] Departamento de Agronomia-CCA, Universidade Estadual de Londrina, 86051–990 Londrina-PR, Brazil
[f] Instituto de Física, Universidade de São Paulo, C.P. 66318, 05315–970, São Paulo, SP, Brazil

ARTICLE INFO

Article history:
Received 16 December 2010
Received in revised form 11 April 2011
Accepted 20 April 2011
Available online 17 May 2011

Keywords:
Fe^{3+}
Ferrihydrite
Hematite
Kaolinite
Quartz

ABSTRACT

Samples of Araucária area soil from Paraná state, Brazil, were separated by particle size fractionation and investigated by electron paramagnetic resonance (EPR) in X-Band of 9.5 GHz at room temperature and 77 K, infra-red spectroscopy and X-ray diffractometry. The paramagnetic species in the soil samples were identified by comparison with EPR spectra of some minerals studied recently by our group, several soil types and/or soil components investigated in the literature. The value of $g = 2.1$ ($\Delta H = 85$ mT) indicated the presence of ferrihydrite. Hematite was identified by $g = 2.1$ ($\Delta H = 100$ mT) and $g = 4.3$ for Fe^{3+} lines of the concentrated dominium and diluted dominium. Kaolinite was identified by IR and EPR with the resonance at $g = 4.3$ attributed to Fe^{3+} ions in isolated sites of tetrahedral and octahedral symmetry with rhombic distortion. The resonances at $g = 3.7$ and $g = 4.9$ were attributed to Fe^{3+} in more highly symmetrical environment than rhombic symmetry, but not in axial symmetry. Three signals around $g = 2$ were attributed to radiation defects, plus additional resonances at $g = 2.8$ and 9.0. Signals less intense than those at $g = 2.1$, 3.7, and 6.5, observed for clear grains of soil, were attributed to presence of Fe^{3+} in quartz which was identified by IR and XDR.

1. Introduction

With the future aim of qualifying and quantifying the contamination in soils exposed to petroleum and oil by-product spillage, EPR, FT-IR and XRD were used to characterize soil paramagnetic species in the area of Araucária, PR, Brazil, more precisely in the proximities of Getúlio Vargas refinery (REPAR/PETROBRAS), a region at great risk of contamination. The soil used in this study was classified as an association of Fluvic Neosoil and Haplic Gleisoil (Thibes-Rodrigues et al., 2006) and is composed of sand, silt and clay, where the minerals such as dolomite and kaolinite are present in these fractions.

The considerable concentration of iron compounds in soils broadens the resonance lines and causes the superposition of lines in the EPR spectra, hindering and frequently impeding the identification of paramagnetic species in the samples (Abragham and Bleaney, 1970). In the present study, the soil fractions (sand: 2 mm–50 μm, silt: 50–2 μm and clay: <2 μm) were separated by particle size fractionation (Hillel, 1998) before these fractions were studied by EPR, FT-IR and XRD techniques.

The paramagnetic species and of certain soil minerals were determined by comparing the spectra with spectra recently investigated by our group and the results obtained by other authors.

2. Materials and methods

2.1. Sample preparation

The soil samples were collected from the surroundings of the Getúlio Vargas refinery (REPAR/PETROBRAS) in the Araucária area (25° 35 12 S and 49° 20 45 W), of the central-southern region of the first plateau of Paraná state, Brazil. The raw soil samples were dried at 380 K for 24 h, sieved and submitted to chemical analysis (Table 1). The soil samples were agitated for 45 min at room temperature and fractionated with the Bertel sieving system (Empresa Brasileira de Pesquisa Agropecuária, 1997). The soil particles were identified according to their minimum and maximum diameters (Table 2), as determined by sieve mesh size; i.e., the size of the grains retained in each sieve. The sample S(>1000) contained grains with maximum diameters of 2 mm. Clear and dark grains were selected by hand and visual examination after the soil had been sieved. Clay and silt fractions were separated by the pipette method (Oliveira et al., 2002).

The crude samples of kaolinite and quartz used for comparison were supplied by Minerais do Paraná SA, MINEROPAR. The hematite

* Corresponding author. Tel./fax: +55 43 3371 4684.
E-mail address: dimauro@uel.br (E. Di Mauro).

0169-1317/$ – see front matter © 2011 Elsevier B.V. All rights reserved.
doi:10.1016/j.clay.2011.04.018

Table 1
Particle size and basic chemical characterization of soil under study.

Properties	Result
pH	5.4
Ca^{2+} ($cmol_c\ dm^{-3}$)	1.9
Mg^{2+} ($cmol_c\ dm^{-3}$)	1.5
K^{+} ($cmol_c\ dm^{-3}$)	0.1
Al^{3+} ($cmol_c\ dm^{-3}$)	0.95
CTC $_{effective}$ ($cmol_c\ dm^{-3}$)	4.45
P ($mg\ dm^{-3}$)	30.0
Cu ($mg\ dm^{-3}$)	0.5
Fe ($mg\ dm^{-3}$)	900
Mn ($mg\ dm^{-3}$)	27
Zn ($mg\ dm^{-3}$)	5.8
Sand %	12
Silt %	39
Clay %	49

and ferrihydrite samples were prepared as described by Schwertmann and Cornell (1991).

2.2. EPR spectroscopy

EPR experiments were performed at the X-band microwave frequency (9.5 GHz) and a magnetic field modulation of 100 kHz with the JEOL (JES-PE-3X) equipment at room temperature and 77 K. A standard sample of MgO:Mn^{2+} (g = 1.981 of the fourth line) was maintained in the EPR cavity, the data were recorded simultaneously with the sample. Samples were introduced into 4 mm quartz EPR tubes that were previously checked for the absence of any spurious signal.

2.3. FT-IR spectroscopy

The IR spectra were recorded on the FT-IR 8300 Shimadzu instrument using pressed KBr disks (10 mg sample and 200 mg KBr). The spectral resolution was 4 cm^{-1}, and each spectrum was obtained after acquiring 90 spectra. The 10 mg of each sample plus 200 mg of KBr were weighed and ground in an agate mortar with a pestle until a homogeneous mixture was obtained. Disc pellets were prepared and the spectra were recorded from 400 to 4000 cm^{-1}. The FT-IR spectra were analyzed using the Origin software (5.0, 2001).

2.4. X-ray diffractometry

The X-ray diffractograms were obtained on the XRD-6000 Shimadzu instrument, using a monochromator (CuKa), the scanning parameters were set at 0.02°2θ, step width, count time 0.6 s from 2 to 70°2θ. The powder samples were placed on a glass slide. X-ray diffractograms were analyzed by the Grams/386 v 4.0 (Galactic Ind. Corp.) software.

Table 2
Nomenclature of the soil samples obtained after straining.

Sample	Retained in the mesh (μm)	Grain diameter d (μm)
S	No retained soil	Various
S(>1000)	1000	d>1000
S(710–1000)	710	710<d<1000
S(500–710)	500	500<d<710
S(355–500)	355	355<d<500
S(180–355)	180	180<d<355
S(90–180)	90	90<d<180
S(<90)	Not retained in any of the meshes	d<90

3. Results and discussion

3.1. EPR spectroscopy

3.1.1. Samples S, S(500–710), S(355–500), S(90–180) and S(<90)

The samples S, S(500–710), S(355–500), S(90–180) and S(<90) presented similar EPR spectra, revealing a resonance at g = 2.1 (Fig. 1). The *g* value is a convenient effective parameter used to locate the spectral positions, defined by the equation $h\nu = g\beta H$, where *h* is Planck's constant, ν is the spectrometer frequency, β is the Bohr magneton, and *H* is the magnitude of the applied magnetic field at resonance. The intense wide resonance line centered at g = 2.1 and with $\Delta H \sim 85$ mT was present in all the EPR spectra was the predominant signal in the spectra of Fig. 1. The EPR signal of the soil samples of Fig. 1 is exactly that of ferrihydrite. This type of signal is very common in soils due to a considerable concentration of Fe^{3+} hydr(oxides), possibly Fe_2O_3, FeO(OH) or Fe5HO$_8$.4H2O, which can form complexes with inorganic matter (Mercê et al., 1996). The small signal with g = 4.3 will be discussed below.

3.1.2. Samples S(>1000), S(710–1000), S(180–355), S(>1000)-dark and S(710–1000)-dark

The paramagnetic species in the samples S(>1000), S(>1000)-dark, S(710–1000), S(710–1000)-dark and S(180–355) (Fig. 2) also presented similar EPR spectra, revealing a resonance at g = 4.3 and another at g = 2.1. These EPR responses were characterized by a relatively weak signal at g = 4.3 of the Fe(III) center of S = 5/2, which could be occupying either a tetrahedral or octahedral site with rhombic distortion, substituting either a 4-fold coordinated silicon of a SiO_4 tetrahedron or a 6-fold coordinated Al^{3+} ion in the kaolinite structure (Bartoll et al., 1996), given that kaolinite, $Al_2[Si_2O_5](OH)_4$, is a crystalline structure consisting of a tetrahedral sheet of oxide-silica composition $[Si_{2n}O_{5n}]^{2n-}$ and an octahedral sheet of aluminum-oxygen-hydrogen composition $[Al_{2n}(OH)_{4n}]^{+}_{2n}$ (Vasyukov et al., 2002).

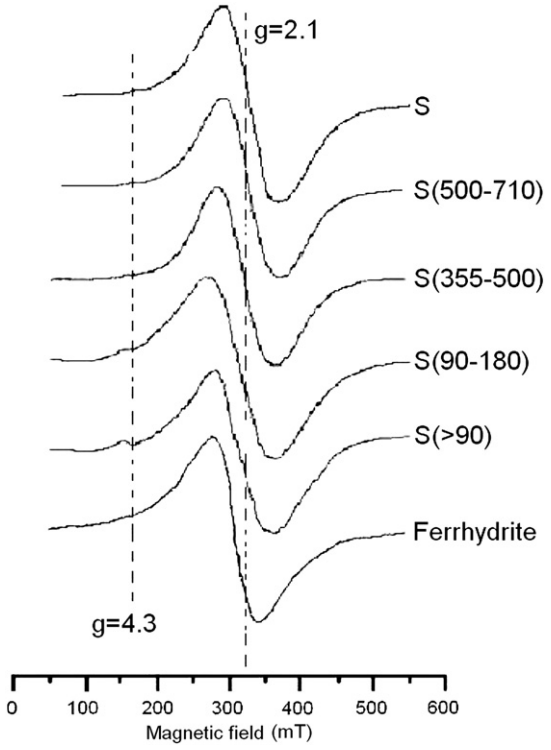

Fig. 1. EPR spectra of soil samples and ferrihydrite at room temperature.

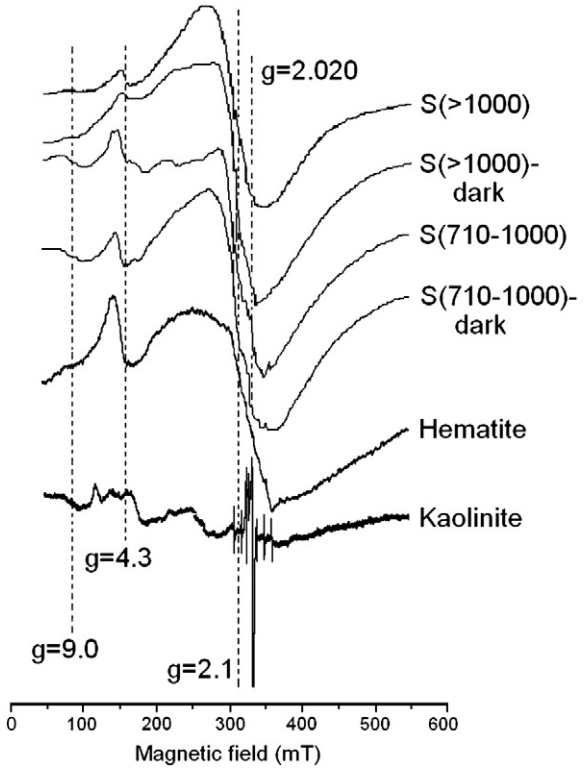

Fig. 2. EPR spectra of soil samples, hematite and kaolinite at room temperature.

This signal is also frequently obtained in clear sands. Besides the signal at g = 4.3, an intense wide resonance line centered at g = 2.1 and with $\Delta H \sim 100$ mT was present in all the EPR spectra. It is evident that the soil samples showed predominantly signals of hematite and kaolinite. The sextet of lines of Mn^{2+} in the kaolinite spectrum (Fig. 2) are not of kaolinite but of the standard sample of MgO:Mn^{2+} in the EPR cavity. The hematite showed resonances at g = 2.1 and g = 4.3 for Fe^{3+} lines of the concentrated dominium and diluted dominium (Ardelean et al., 2001). Additional resonances at g = 9.0 and around g = 2 in the spectra are characteristic lines of kaolinite (Fig. 2).

The origin of the g ~ 2 EPR lineshape was attributed to the ferromagnetic resonance (FMR) (Griscom, 1984) of the super-paramagnetic centers of small single domains. These can be understood as resulting from exchange interactions, dimmers and other dark grains that can agglomerate in sizes consisting of a few nanoparticles and that contain crystalline phases of single domains of iron hydr(oxides) and/or other species. Sand can also appear in the form of gray grains (Teixeira et al., 2000) or as agglomerates, a fact that maintained a stronger EPR signal at g = 4.3 (Fig. 2). The iron EPR lines can be compared with the EPR spectra of silicate glasses doped with Mn^{2+} (Baesso et al., 1989) because both ions present similar magnetic interactions for isolated and agglomerated ions. Considerable quantities of sand grains were verified in the soil samples containing grains > 0.7 mm (Teixeira et al., 2000) (Fig. 2). A similar behavior was shown in the EPR spectral components of Cr^{3+} at barium alumino-borate and silicate glass sites (g = 5.25 and 1.97) (Karapetyan et al., 1965; Landry et al., 1967; O´Reilly and MacIver, 1962; Pontuschka et al., 2001) in close analogy to Fe^{3+} (Castner et al., 1960; Loveridge and Parke, 1971) in silicate and borate glasses (g = 9.3, 4.3 and 2.0). When a pair or many of such ions are associated in dimmers or clusters, the exchange interaction plays an important role giving rise to a broad ferromagnetic resonance at g ~ 2 (Griscom, 1984; Karapetyan et al., 1965; Landry et al., 1967; Pontuschka et al., 2001).

3.1.3. Samples S(>1000)-clear and S(710–1000)-clear

Soils rich in quartz and poor in iron oxides present clear whitish colors (Azevedo and Dalmolin, 2004). The EPR spectra of S(>1000)-clear and S(710–1000)-clear colored soil samples at room temperature (Fig. 3) indicated a lower amount of iron ferromagnetic resonance (broad line at g ~ 2) and a relatively stronger line at g = 3.7, compared to the EPR spectra of the other samples (Figs. 1 and 2). The comparison of the spectra indicated that the paramagnetic species in the soil samples were quartz and kaolinite. The samples S(>1000)-clear and S(710–1000)-clear, in agreement with particle size and color, were classified as sand (Teixeira et al., 2000). Their spectra were comparable to the spectra of sand and sandy soil (Drummond et al., 2001; Lombardi et al., 2002). The spectra of the sand revealed a lower concentration of iron hydr(oxides). In clear samples like sand or kaolinite, Fe^{3+} occurs in tetrahedral and/or octahedral substitution, whereas in darker samples, single ferri- or ferromagnetic domains exhibit super-paramagnetic behavior (Griscom, 1984) in sand and in soil. The sand presented smaller quantities of iron hydr(oxides) than the soils. In the sample S(>1000)-clear (Fig. 3), EPR lines occurred at g = 4.9 and 3.7, due to the substitution of Al^{3+} for Fe^{3+} in kaolinite in axial symmetry, resulting in superposed signals (Drummond et al., 2001; Gaite et al., 1993). Usually, these lines are not detected in the EPR spectra of most soils due to the superposition of iron hydr(oxides) resonances (Mestdagh et al., 1980) (Figs. 1 and 2). The soil samples of Fig. 3 exhibited additional resonances at g = 2.020, 2.8 and 4.3, also present in the kaolinite spectra. In Fig. 3, beyond the paramagnetic species mentioned above, three other signals with resonances at g = 2.1, 3.7 and 6.5 were identified. The corresponding species were also present in quartz and probably due to the fact that the lightest part of the soil contains certain amounts of quartz.

3.1.4. Samples S(710–1000) and S(710–1000)-dark at 77 K

The EPR spectra of the samples S(710–1000)-dark, S(710–1000), hematite, and kaolinite at 77 K are shown in Fig. 4. The FMR signal intensity of the iron hydr(oxides) (g = 2.1) was reduced relative to the intensity of the Fe^{3+} signal (g = 4.3), as observed for hematite and kaolinite. The same observation was made by Bensimon et al. (1999), and was explained by a modification of the super-paramagnetic character of iron nanoparticles when the temperature was reduced.

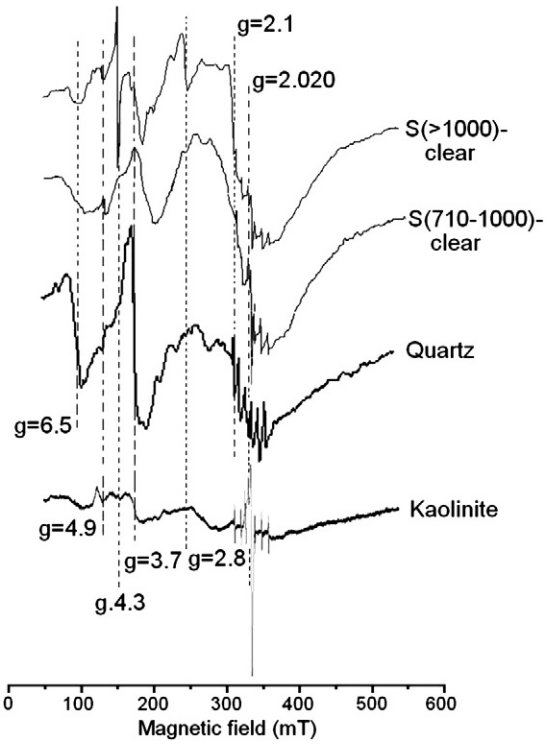

Fig. 3. EPR spectra of soil samples, kaolinite and quartz at room temperature.

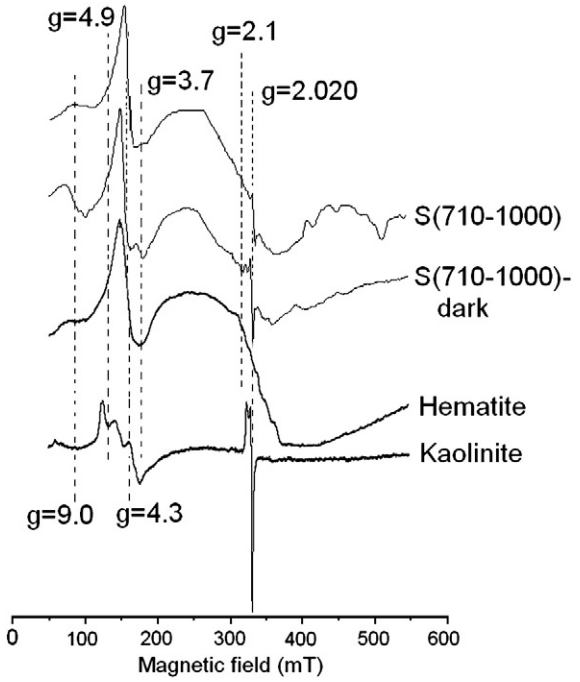

Fig. 4. EPR spectra of soil samples at 77 K.

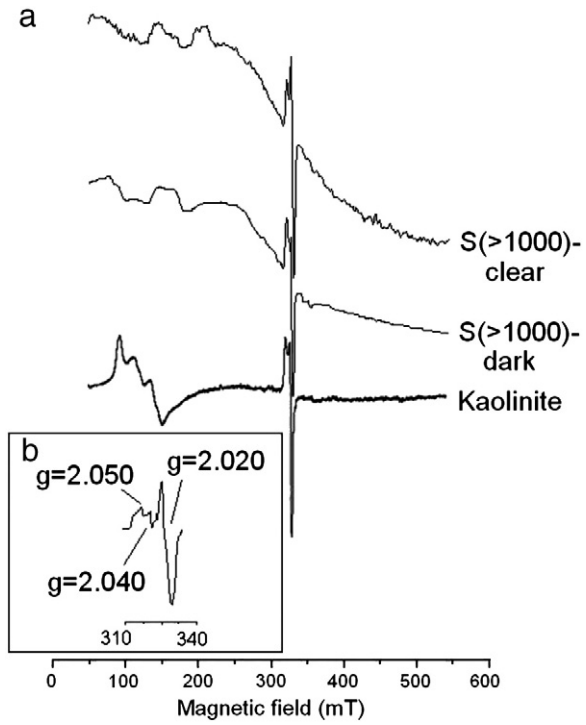

Fig. 5. EPR spectra of soil samples at 77 K: a) S(>1000)-clear and S(>1000)-dark samples; b) (inset) S(>1000)-dark sample with the magnetic field centered around 330 and a 20 mT sweep.

Fig. 4 clearly shows the signals of the paramagnetic species of the kaolinite and hematite with g = 4.3, and additional resonances at g = 3.7, 4.9, and 9.0. The defect signals around g = 2 are discussed below.

3.1.5. Samples S(>1000)-clear and S(>1000)-dark at 77 K

At 77 K, the EPR lines of S(>1000) around g = 2.02 and 2.05 were clearly visible due to the attenuation of the intensity of the line at g = 2.1 as mentioned above. The EPR lines at g = 2.02 and 2.05 were of the same characteristics in the soil spectra but in the majority, these lines were superposed by the resonance at g = 2.1, attributed to the ferromagnetic resonance of the iron hydr(oxides). These lines (Fig. 5a) were found in the majority of the soil spectra and were attributed to defects in the centers of the silicium-oxygen tetrahedra and aluminum-oxygen octahedra in kaolinite (Meads and Malden, 1975; Muller and Calas, 1993). These defects cause the different intensities in the EPR lines of the soils at g = 2.05, 2.04 and 2.02, varying according to the amount of the species in each sample. The possible defects are Center A (center $Si–O^-$ in orthorhombic symmetry with $g_z = 2.0490 \pm 0.0005$, $g_y = 2.006 \pm 0.001$ and $g_x = 2.001 \pm 0.001$), Center A (center $Si–O^-$ in axial symmetry with $g_{//} = 2.039 \pm 0.002$ and $g_{\perp} = 2.008 \pm 0.001$) and Center B (one electron missing from the $Al_{vi}–O^–Al_{vi}$ bridge, with $g_1 = 2.040 \pm 0.0005$, $g_2 = 2.020 \pm 0.0005$ and $g_3 = 2.002 \pm 0.001$) (Clozel et al., 1994).

The spectrum of the same sample but with the magnetic field centered at 330 and with a 20 mT sweep is shown in Fig. 5b (as inset). The sample S(>1000)-dark at 77 K (Fig. 5b) showed the centers A and B and possibly center A . It was not possible to guarantee the presence of the Center A' since it exists near to the values $g_{//} = 2.039$ and $g_1 = 2.040$, and these are within experimental uncertainty or are revealed as superposed lines.

Manganese, usually present in soil samples, was not detected in the spectra of samples S(<1000)-dark. This could be due to the fact that Fe^{3+} showed an intense wide EPR line which is superposed by the manganese lines (Ceretta et al., 1999) since Mn^{2+} associated with organic matter shows interaction that broadens the signal and, consequently, the EPR line disappears (Moreira et al., 2006). McBride (1989) verified the loss of the EPR signal of Mn^{2+} due to the considerable line width enlargement caused by very stable bonds of Mn^{2+} with carboxylic acids.

3.2. FT-IR and XRD

3.2.1. Samples S, S(500–710), S(355–500), S(90–180) and S(<90)

The FT-IR spectra of S, S(500–710), S(355–500), S(90–180) and S(<90) (Fig. 6) showed the characteristic bands of quartz, kaolinite and 2:1 clay minerals. The minerals 2:1 and quartz were also observed in the diffractograms (Fig. 7a and b). The characteristic XRD reflections of kaolinite were not observed because the higher intensity of the quartz reflections. Due to the higher intensity of the IR bands of the quartz and clay minerals, the characteristic bands of the iron hydr (oxides) were not visible. Characteristic bands of quartz were found at

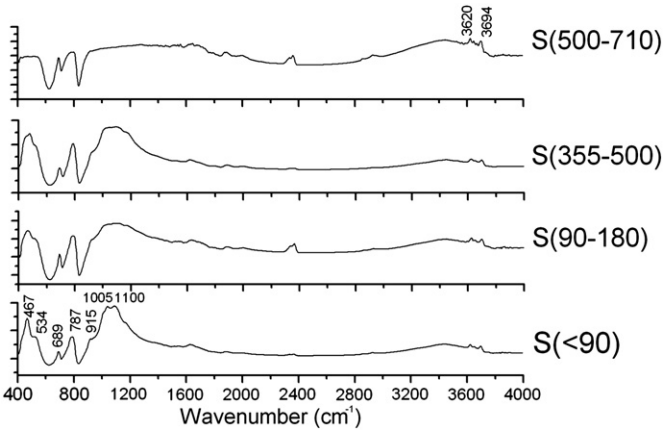

Fig. 6. Infrared spectra of samples S, S(500–710), S(355–500), S(90–180) and S(<90).

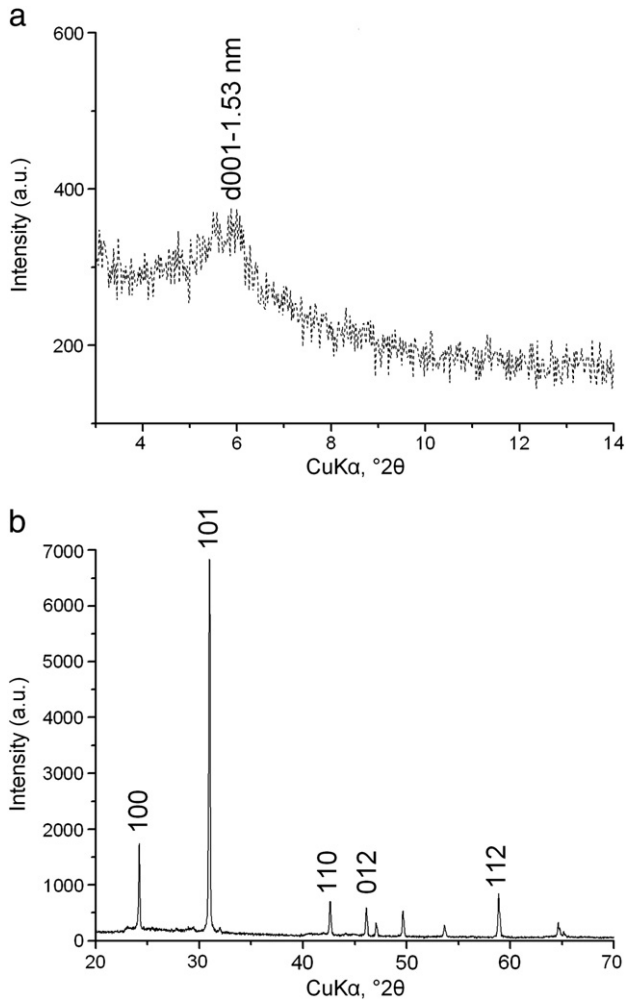

Fig. 7. X-ray diffractograms and the basal reflection of the S(>1000) fraction: a) clay minerals; b) quartz.

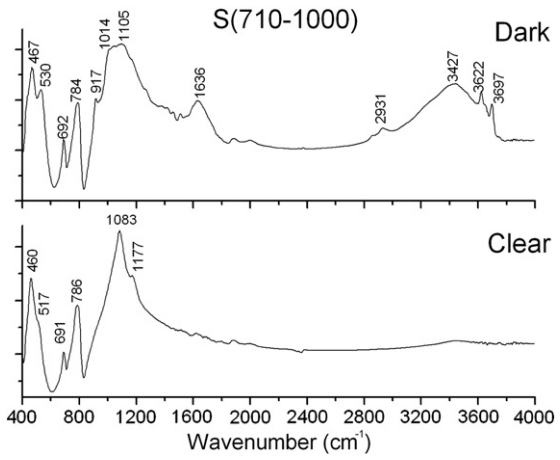

Fig. 8. Infrared spectra of samples S, S(710–1000)-dark fraction and S(710–1000)-clear.

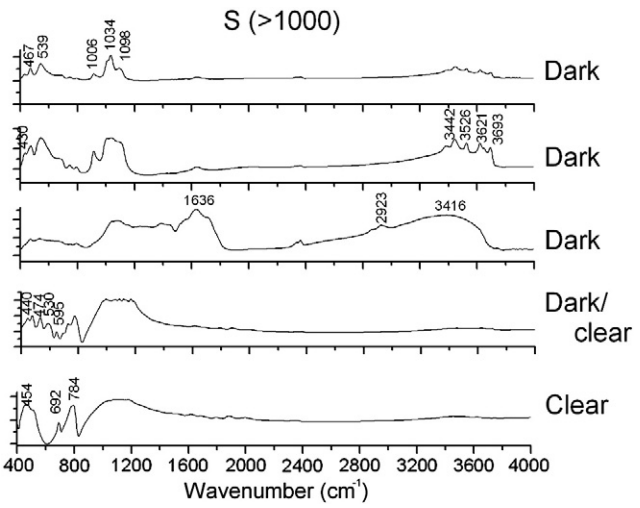

Fig. 9. Infrared spectra of samples S, S(>1000)-dark fraction and S(>1000)-clear.

460–1186 cm^{-1} (which can be attributed to Si–O–Si and Si–O in tetrahedral sites). The bands of clay minerals were observed at 429–1112 cm^{-1} (which can be attributed to Si–O bending vibrations, Al–OH stretching vibration, Si–O in and out of the deformation plane). At 3395–3694 cm^{-1} the OH stretching bands of the structural hydroxyl groups and the water molecules were visible. The typical bands at 3620 and 3694 cm^{-1} were related the stretching vibration of internal OH groups in kaolinite and the vibration bands of surface of OH groups (Fukamachi et al., 2007).

3.2.2. Samples S(>1000) and S(710–1000)

The dark grains samples contained quartz, kaolinite and 2:1 clay minerals (Fig. 8). The band at 1636 cm^{-1} could be attributed to COOH of organic matter and at 2931 cm^{-1} to the C–H symmetric stretching vibration of g CH_3 groups (Miranda et al., 2007).

Like the former samples, the spectra of S(>1000) indicated also quartz, kaolinite and 2:1 clay minerals. The iron hydr(oxides) were identified by the bands at 430, 467 and 530–539 cm^{-1} which represent Fe–O bonds (Fig. 9).

4. Conclusions

The EPR spectra of soil samples from Araucária-PR presented ferromagnetic resonance lines at g = 2.1 due to large concentrations of Fe^{3+} hydr(oxides), possibly ferrihydrite (ΔH = 85 mT) or hematite (ΔH = 100 mT) which may interact with inorganic matter and organic components. The hematite showed an additional resonance at g = 4.3. Kaolinite was identified by IR and EPR with the resonance at g = 4.3 attributed to Fe^{3+} ions in isolated sites of tetrahedral and octahedral symmetries with rhombic distortion. Resonances at g = 3.7 and 4.9 were attributed to Fe^{3+} in structures with higher symmetry than rhombic symmetry, but not in axial symmetry. Defects in the kaolinite structure were detected by EPR spectra (centers A, B and possibly center A) but the superposition of the EPR lines impeded the precise identification of the paramagnetic center A–. EPR at the Q- or W-band could be useful for clearer characterization of this possible center. The three signals of the kaolinite around g = 2 were attributed to radiation defects. Kaolinite showed also additional resonances at g = 2.8 and 9.0. The clear grains of the soils showed intense signals at g = 2.1, 3.7, 6.7 due to presence of Fe^{3+} in quartz. Thus, after particle size separation, EPR spectroscopy together with complementary techniques (FT-IR and XDR) can be used to characterize even complex and heterogeneous soil systems.

Acknowledgements

The authors would like to thank the Brazilian petroleum company, PETROBRAS, for supplying the soil samples, the Minerais do Paraná SA, MINEROPAR, for supplying the mineral samples, and the "Coordenação

de Aperfeiçoamento de Pessoal de Nível Superior" (CAPES-Brazil) for financial support through fellowship grants.

References

Abragham, A., Bleaney, B., 1970. Electron Paramagnetic Resonance of Transition Ions. Clarendon Press, Oxford.

Ardelean, I., Peteanu, M., Simon, V., Ciorcas, F., Ioncu, V., 2001. Structural investigation of Fe_2O_3–TeO_2–B_2O_3–SrO glasses by EPR. J. Materials Science Letters 20, 947–949.

Azevedo, A.C., Dalmolin, R.S.D., 2004. Solos e Ambiente: Uma Introdução. Palotti - UFSM, Santa Maria, RS.

Baesso, M.L., Mansanares, A.M., Silva, E.C., Vargas, H., 1989. Phase-resolved Photo-acoustic spectroscopy and EPR investigation of MnO_2 and CoO doped soda-lime glasses. Physical Review B 40, 1880–1884.

Bartoll, J., Tani, A., Ikeya, M., Inada, T., 1996. ESR investigations of burnt soil. Applied Magnetic Resonance 11, 577–586.

Bensimon, Y., Deroide, B., Zanchetta, J.V., 1999. Comparison between the Electron Paramagnetic Resonance spectra obtained in X-band and W-band on fired clay: a preliminary study. J. Physics Chemistry Solids 60, 813–818.

Castner Jr., T., Newell, G.S., Holton, W.C., Slichter, C.P., 1960. Note on the paramagnetic resonance of iron in glass. J. Chem. Phys. 32, 668–673.

Ceretta, C.A., Bayer, C., Dick, D.P., Martin-Neto, L., Colnago, L.A., 1999. Métodos espectroscópicos. In: Santos, G.A., Camargo, F.A.O. (Eds.), Fundamentos da matéria orgânica do solo: ecossistemas tropicais e subtropicais. Gênesis, Porto Alegre, RS, pp. 293–336.

Clozel, B., Allard, T., Muller, J.P., 1994. Nature and stability of radiation-induced defects in natural kaolinites — new results and a reappraisal of published works. Clays Clay Minerals 42, 657–666.

Drummond, A.F., Varajão, C., Gilkes, R.J., Hart, R.D., 2001. The relationships between Kaolinite crystal properties and the origin of materials of a Brazilian kaolin deposit. Clays Clay Minerals 49, 44–59.

Empresa Brasileira de Pesquisa Agropecuária, 1997. Manual de métodos de análise de solo, 2ed. Rio de Janeiro. 213p.

Fukamachi, C.R.B., Wypych, F., Mangrich, A.S., 2007. Fe^{3+} ion probe to study the stability of urea-intercalated kaolinite by electron paramagnetic resonance. J. Colloid Interface Sci. 313, 537–541.

Gaite, J.M., Ermakoff, P., Muller, J.P., 1993. Characterization and origin of two Fe^{3+} spectra in kaolinite. Physics Chemistry Minerals 20, 242–247.

Griscom, D.L., 1984. Ferromagnetic resonance of precipitated phases in natural glasses. J. NonCryst. Solids 67, 81–118.

Hillel, D., 1998. Environmental soil physics. Academic Press, San Diego. pp 60–63.

Karapetyan, G.O., Kovalyov, V.P., Lunter, S.G., 1965. Chromium sensitization of the neodymium luminescent solar concentrators. Opt. Spectroscopy 19, 529–531.

Landry, R.J., Fournier, J.T., Young, C.G., 1967. Electron spin resonance and optical absorption studies of Cr^{3+} in a phosphate glass. J. Chem. Phys. 46, 1285–1290.

Lombardi, K.C., Guimarães, J.L., Mangrich, A.S., Mattoso, N., Abbate, N., Schreiner, W.H., Wypych, F., 2002. Structural and morphological characterization of the PP-0559 Kaolinite from the Brazilian Amazon Region. J. Brazilian Chemical Society 13, 270–275.

Loveridge, D., Parke, S., 1971. Electron spin absorption of Fe^{3+}, Mn^{2+} and Cr^{3+} in glasses. Phys. Chem. Glasses 12, 19–27.

Mcbride, M.B., 1989. Surface chemistry of soil minerals, In: Dixon, J.B., Weed, S.B. (Eds.), Minerals in soil environments, 2nd Edition. SSSA Book Series, Madison, WI, US, pp. 35–88.

Meads, R.E., Malden, P.J., 1975. Electron spin resonance in natural kaolinites containing Fe^{3+} and other transition metal ions. Clay Minerals 10, 313–345.

Mercê, A.L.R., Mangrich, A.S., Szpoganicz, B., Levy, N.M., Felcman, J., 1996. Equilibrium studies of Al (III) And Fe(III) with nitrosalicyclic acids — nitrohumic acid-like models. J. Brazilian Chemical Society 7, 97–102.

Mestdagh, M.M., Vielvoye, L., Herbillon, A.J., 1980. Iron in kaolinite: II. Relationship between Kaolinite crystallinity and iron content. Clay Minerals 15, 1–13.

Miranda, C.C., Canellas, L.P., Nascimento, M.T., 2007. Caracterização da matéria orgânica do solo em fragmentos de mata atlântica e em plantios abandonados de eucalipto. Revista Brasileira de Ciência do Solo 31, 905–916.

Moreira, S.G., Prochnow, L.I., Kiehl, J.C., Martin-Neto, L., Pauletti, V., 2006. Formas químicas, disponibilidade de manganês e produtividade de soja em solos sob semeadura direta. Obtainable from Revista Brasileira de Ciência do Solo 30. http://www.scielo.br/scielo.php?pid=S0100-06832006000100013&script=sci_arttext.

Muller, J.P., Calas, G., 1993. Genetic significance of paramagnetic centers in kaolinites. In kaolin genesis and utilization Special Pub. The Clay Minerals Society 84, 261–289.

O´Reilly, D.E., MacIver, D.S., 1962. Electron Paramagnetic Resonance absorption of Chromia-alumina Catalystis. J. Phys. Chem. 66, 276–281.

Oliveira, G.C., Dias Junior, M.S., Vitorino, A.C.T., Ferreira, M.M., Sá, M.A.C., Lima, J.M., 2002. Agitador horizontal de movimentos helicoidal na dispersão mecânica de amostras de três Latossolos do sul e campos das vertentes de Minas Gerais. Ciência Agrotécnica 26, 881–887.

Pontuschka, W.M., Kanashiro, L.S., Courrol, L.C., 2001. Luminescence mechanisms for borate glasses: the role of local structural units (invited paper). Fizika i Khimiya Stekla 27, 54–69. Glass Physics Chemistry 27, 37–47.

Schwertmann, U., Cornell, R.M., 1991. Iron Oxides in the Laboratory — Preparation and Characterization. Verlagsgesells chat, Weinheim. p 137.

Teixeira, W., Toledo, M.C.M., Fairchild, T.R., Taioli, F., 2000. Decifrando a Terra. Oficina de Textos, São Paulo, SP.

Thibes-Rodrigues, T., Wisniewski, C., Bona, C., Dedecek, R.A., Santos, G.O., 2006. Caracterização nutricional de branquilho (Sebastiania commersoniana (Baillon) Smith & Downs — Euphorbiaceae). Obtainable from Cultivado em solo contaminado por petróleo. : Floresta, 36. 3, pp. 349–359http://ojs.c3sl.ufpr.br/ojs2/index.php/floresta/article/viewFile/7514/5375.

Vasyukov, V.N., Shapovalov, V.V., Schwarz, S.A., Ravailovich, M.H., Sokolov, J., Cbeloshenko, V.A., 2002. Temperature-induced changes in the EPR spectrum of the magnetic center in kaolin. J. Magn. Reson. 154, 15–21.